articles

molecular pharmaceutics

Combination Chemotherapy and Photodynamic Therapy with Fab′ Fragment Targeted HPMA Copolymer Conjugates in Human Ovarian Carcinoma Cells

Jarunee Hongrapipat,[†,‡] Pavla Kopečková,[†] Jihua Liu,[†] Sompol Prakongpan,[‡] and Jindřich Kopeček*[,†,§]

Department of Pharmaceutics and Pharmaceutical Chemistry and Department of Bioengineering, University of Utah, Salt Lake City, Utah 84112, and Department of Pharmacy, Mahidol University, Bangkok 10400, Thailand

Received January 9, 2008; Revised Manuscript Received July 13, 2008; Accepted July 14, 2008

Abstract: The biological activities of sequential combinations of anticancer drugs, SOS thiophene (SOS) and mesochlorin e_6 monoethylenediamine (Mce_6), in the form of free drugs, nontargeted *N*-(2-hydroxypropyl)methacrylamide (HPMA) copolymer−drug conjugates, P-GFLG-Mce_6 and P-GFLG-SOS (P is the HPMA copolymer backbone and GFLG is the glycylphenylalanylleucylglycine spacer), and Fab′-targeted HPMA copolymer−drug conjugates, P-(GFLG-Mce_6)-Fab′ and P-(GFLG-SOS)-Fab′ (Fab′ from OV-TL16 antibodies complementary to CD47), were evaluated against human ovarian carcinoma OVCAR-3 cells. Mce_6, SOS, P-GFLG-Mce_6, P-GFLG-SOS, P-(GFLG-Mce_6)-Fab′, and P-(GFLG-SOS)-Fab′, when used as single agents or in binary combination, exhibited cytotoxic activities against OVCAR-3 cells, as determined using a modified MTT assay. The binding and internalization of P-(GFLG-Mce_6)-Fab′ and P-(GFLG-SOS)-Fab′ by OVCAR-3 cells were visualized by confocal microscopy and flow cytometry. The results confirmed an enhanced biorecognition by OVCAR-3 cells of Fab′-targeted HPMA copolymer conjugates over nontargeted conjugates. The median-effect analysis and the determination of the combination index (CI) were used to describe the drug interaction and quantify the synergism, antagonism, or additivity in anticancer effects. The sequential combinations of SOS+Mce_6 and P-GFLG-SOS+P-GFLG-Mce_6 displayed very strong synergism to synergism in the entire range of cell inhibition levels ($f_a = 0.5 - 0.95$). The P-(GFLG-SOS)-Fab′+P-(GFLG-Mce_6)-Fab′ exhibited a strong synergism for f_a values up to about 0.85, but showed synergistic effect and nearly additive effect at $f_a = 0.9$ and 0.95, respectively. These observations support the continuation of *in vivo* investigations of these conjugates for the treatment of ovarian cancer.

Keywords: *N*-(2-Hydroxypropyl)methacrylamide (HPMA) copolymer; Fab′ antibody fragment; 2,5-*bis*(5-hydroxymethyl-2-thienyl)furan; mesochlorin e_6 monoethylenediamine; combination index; ovarian cancer

Introduction

Polymer−drug conjugates are established as one of the first-generation nanomedicines for the treatment of cancer. Their use facilitates the uptake and transport of therapeutic agents and creates a dose-differentiation between the treatment target and the rest of the body, due to the fact that macromolecules can accumulate passively in solid tumor tissue by the phenomenon called "enhanced permeability and retention (EPR) effect".[1] The enhanced drug accumulation in tumor tissue increases the

* To whom correspondence should be addressed. Mailing address: Department of Pharmaceutics and Pharmaceutical Chemistry, University of Utah, 30 S., 2000 E., Rm. 201, Salt Lake City, UT 84112. Phone: (801) 581-7211. Fax: (801) 581-7848. E-mail: jindrich.kopecek@utah.edu.

† Department of Pharmaceutics and Pharmaceutical Chemistry, University of Utah.

‡ Mahidol University.

§ Department of Bioengineering, University of Utah.

(1) Maeda, H.; Seymour, L. W.; Miyamoto, Y. Conjugates of anticancer agents and polymers: advantages of macromolecular therapeutics in vivo. *Bioconjugate Chem.* **1992**, *3* (5), 351–362.

(2) Breunig, M.; Bauer, S.; Goepferich, A. Polymers and nanoparticles: intelligent tools for intracellular targeting? *Eur. J. Pharm. Biopharm.* **2008**, *68* (1), 112–128.

10.1021/mp800006e CCC: $40.75
Published on Web 08/27/2008

therapeutic effect while reducing nonspecific side-effects.[2−4] Moreover, the intracellular trafficking mechanism of polymer−drug conjugates renders drug efflux pumps ineffective.[5] To obtain such multifunctional capabilities, polymer−drug conjugates have been designed to consist of (a) a nonimmunogenic and biocompatible water-soluble polymer backbone such as poly(ethylene glycol) or *N*-(2-hydroxypropyl)methacrylamide (HPMA) copolymers,[6] (b) therapeutically active molecules, (c) linkers between the polymer backbone and the active molecule that are stable in blood circulation and release the free drug at target sites, and (d) a targeting moiety to mediate biomolecular recognition.[7,8] HPMA copolymers are one of the most frequently evaluated polymer backbones in polymer−drug conjugates. The main advantages of HPMA copolymer−drug conjugates over their low molecular weight drugs (reviewed in Kopeček,[6] Putnam and Kopeček,[8] Kopeček et al.,[5] Duncan,[9] Cuchelkar and Kopeček,[10] Pan and Kopeček[11]) include the following: (1) enhanced water solubility of poorly soluble or insoluble drugs with concomitant improvement of drug bioavailability; (2) long-lasting circulation in the bloodstream;[12,13] (3) decreased nonspecific toxicity of the conjugated drug and immunogenicity of the targeting moiety;[14] (4) increased *passive* and/or *active* accumulation of the drug at the site of its action by the EPR effect and/or by targeting, respectively;[15−17] (5) active uptake by fluid-phase pinocytosis (nontargeted polymer-bound drug) or receptor-mediated endocytosis (targeted polymer bound drug); (6) the potential to overcome efflux pump-mediated mechanism of drug resistance;[18−20] and (7) ability to deliver several active components with different properties to the same target site that enhance the specific activity of the main drug.[21,22] The incorporation of targeting moieties, such as monoclonal antibody (mAb) or antibody fragment, into HPMA copolymer−drug conjugates results in specific delivery and enhancement of the amount of the polymeric conjugate being internalized by receptor-mediated endocytosis.[23] Consequently, the intracellular concentration of the polymeric conjugates is enhanced with concomitant increase in antitumor activity.[17] Moreover, the polymer modification of mAb or antibody fragments reduces their immunogenicity and extends their circulating half-lives.[14,24] The use of antibody fragments provides a better control of the structure of HPMA copolymer conjugates compared to full-length mAb. The unique sulfhydryl group near the C terminus of Fab′ fragments has provided a convenient way for coupling to HPMA copolymers containing maleimide groups and allow the antigen-binding site to be more approachable.[25,26]

(3) Duncan, R. Polymer conjugates as anticancer nanomedicines. *Nat. Rev. Cancer* **2006**, *6* (9), 688–701.

(4) Kiick, K. L. Materials science. Polymer therapeutics. *Science* **2007**, *317* (5842), 1182–1183.

(5) Kopeček, J.; Kopečková, P.; Minko, T.; Lu, Z. HPMA copolymer-anticancer drug conjugates: design, activity, and mechanism of action. *Eur. J. Pharm. Biopharm.* **2000**, *50* (1), 61–81.

(6) Kopeček, J. Soluble biomedical polymers. *Polim. Med.* **1977**, *7* (3), 191–221.

(7) Khandare, J.; Minko, T. Polymer−drug conjugates: Progress in polymeric prodrugs. *Prog. Polym. Sci.* **2006**, *31*, 359–397.

(8) Putnam, D.; Kopeček, J. Polymer Conjugates with Anticancer Activity. *Adv. Polym. Sci.* **1995**, *122*, 55–123.

(9) Duncan, R. The dawning era of polymer therapeutics. *Nat. Rev. Drug Discovery* **2003**, *2* (5), 347–360.

(10) Cuchelkar, V.; Kopeček, J. Polymer−Drug Conjugates. In *Polymers in Drug Delivery*; Uchegbu, I. F., Schätzlein, A. G., Eds.; CRC Press: Boca Raton, FL, 2006; pp 155−182.

(11) Pan, H.; Kopeček, J. Multifunctional Water-Soluble Polymers for Drug Delivery. In *Multifunctional Pharmaceutical Nanocarriers*; Torchilin, V. P., Ed.; Springer: New York, 2008; pp 81−142.

(12) Seymour, L. W.; Duncan, R.; Strohalm, J.; Kopeček, J. Effect of molecular weight (Mw) of *N*-(2-hydroxypropyl)methacrylamide copolymers on body distribution and rate of excretion after subcutaneous, intraperitoneal, and intravenous administration to rats. *J. Biomed. Mater. Res.* **1987**, *21* (11), 1341–1358.

(13) Seymour, L. W.; Ulbrich, K.; Strohalm, J.; Kopeček, J.; Duncan, R. The pharmacokinetics of polymer-bound adriamycin. *Biochem. Pharmacol.* **1990**, *39* (6), 1125–1131.

(14) Říhová, B.; Kopečková, P.; Strohalm, J.; Rossmann, P.; Větvička, V.; Kopeček, J. Antibody-directed affinity therapy applied to the immune system: in vivo effectiveness and limited toxicity of daunomycin conjugated to HPMA copolymers and targeting antibody. *Clin. Immunol. Immunopathol.* **1988**, *46* (1), 100–114.

(15) Lu, J. M.; Peterson, C. M.; Guo-Shiah, J.; Gu, Z. W.; Peterson, C. A.; Straight, R. C.; Kopeček, J. Cooperativity between free and *N*-(2-hydroxypropyl)methacrylamide copolymer bound adriamycin and meso-chlorin e_6 monoethylene diamine induced photodynamic therapy in human epithelial ovarian carcinoma in vitro. *Int. J. Oncol.* **1999**, *15* (1), 5–16.

(16) Shiah, J. G.; Dvořák, M.; Kopečková, P.; Sun, Y.; Peterson, C. M.; Kopeček, J. Biodistribution and antitumour efficacy of long-circulating *N*-(2-hydroxypropyl)methacrylamide copolymer-doxorubicin conjugates in nude mice. *Eur. J. Cancer* **2001**, *37* (1), 131–139.

(17) Shiah, J. G.; Sun, Y.; Kopečková, P.; Peterson, C. M.; Straight, R. C.; Kopeček, J. Combination chemotherapy and photodynamic therapy of targetable *N*-(2-hydroxypropyl)methacrylamide copolymer-doxorubicin/mesochlorin e_6 - OV-TL 16 antibody immunoconjugates. *J. Controlled Release* **2001**, *74* (1−3), 249–253.

(18) Minko, T.; Kopečková, P.; Kopeček, J. Chronic exposure to HPMA copolymer-bound adriamycin does not induce multidrug resistance in a human ovarian carcinoma cell line. *J. Controlled Release* **1999**, *59* (2), 133–148.

(19) Minko, T.; Kopečková, P.; Kopeček, J. Efficacy of the chemotherapeutic action of HPMA copolymer-bound doxorubicin in a solid tumor model of ovarian carcinoma. *Int. J. Cancer* **2000**, *86* (1), 108–117.

(20) Minko, T.; Kopečková, P.; Pozharov, V.; Kopeček, J. HPMA copolymer bound adriamycin overcomes MDR1 gene encoded resistance in a human ovarian carcinoma cell line. *J. Controlled Release* **1998**, *54* (2), 223–233.

(21) Greco, F.; Vicent, M. J.; Penning, N. A.; Nicholson, R. I.; Duncan, R. HPMA copolymer-aminoglutethimide conjugates inhibit aromatase in MCF-7 cell lines. *J. Drug Targeting* **2005**, *13* (8−9), 459–470.

(22) Vicent, M. J.; Greco, F.; Nicholson, R. I.; Paul, A.; Griffiths, P. C.; Duncan, R. Polymer therapeutics designed for a combination therapy of hormone-dependent cancer. *Angew. Chem., Int. Ed.* **2005**, *44* (26), 4061–4066.

(23) Allen, T. M. Ligand-targeted therapeutics in anticancer therapy. *Nat. Rev. Cancer* **2002**, *2* (10), 750–763.

(24) Chapman, A. P. PEGylated antibodies and antibody fragments for improved therapy: a review. *Adv. Drug Delivery Rev.* **2002**, *54* (4), 531–545.

To improve the therapeutic outcome and reduce the toxicity of anticancer agents, a novel concept of combining chemotherapy and photodynamic therapy (PDT), using HPMA copolymer bound drugs, was developed.[27] The *in vivo* studies on two cancer models, Neuro 2A neuroblastoma induced in A/J mice[28] and human ovarian carcinoma heterotransplanted in nude mice,[17,29,30] demonstrated that combination therapy with HPMA copolymer-bound DOX (doxorubicin) and HPMA copolymer-bound Mce_6 (mesochlorin e_6 monoethylenediamine) produced tumor cures which could not be obtained with either chemotherapy or PDT alone. Furthermore, significantly lower nonspecific toxicities were observed when compared to low molecular weight drugs. Previously, *in vitro* studies of the binary combination of free and HPMA copolymer-bound SOS [2,5-bis(5-hydroxymethyl-2-thienyl)furan, NSC 652287], DOX, and Mce_6 in the treatment of human A498 renal carcinoma cells using the median-effect method showed that these combinations displayed synergistic-to-additive effects, depending on the cytotoxic mechanisms of each agent.[31]

In the present study, Fab′-targeted and nontargeted HPMA copolymer−drug (SOS and Mce_6) conjugates for combination chemotherapy and PDT against human ovarian OVCAR-3 carcinoma cells were synthesized. SOS, a dithiophene compound, was used as the chemotherapy agent. Its mechanism of action consists of disrupting the p53-HDM-2 (human double minute-2) interaction, resulting in an increased p53 accumulation, thereby inducing cell cycle arrest and apoptosis.[32−35] For PDT the second-generation synthetic photosensitizer, Mce_6, was used. Photosensitizer molecules can be activated by specific wavelength of light and interact with molecular oxygen to produce reactive singlet oxygen, causing irreversible photodamage to cells resulting in cell death.[36] The antibody Fab′ fragment was prepared from OV-TL16 antibody, which recognizes the OA-3 surface antigen, also known as CD47 or IAP (integrin-associated protein),[37,38] overexpressed on most human ovarian carcinoma cells.[39,40]

It was hypothesized that a combination of these agents may produce synergistic effects and has higher efficiency than each agent alone. Accordingly, the efficiency of free, nontargeted, and Fab′ fragment-targeted HPMA copolymer-bound SOS and Mce_6 against OVCAR-3 cells as single agents and in combination was evaluated. The combination index (CI) analysis was used to quantify the synergism, antagonism, and additive effects of drug combinations.[41−43]

(25) Lu, Z. R.; Kopečková, P.; Kopeček, J. Polymerizable Fab′ antibody fragments for targeting of anticancer drugs. *Nat. Biotechnol.* **1999**, *17* (11), 1101–1104.

(26) Lu, Z. R.; Shiah, J. G.; Sakuma, S.; Kopečková, P.; Kopeček, J. Design of novel bioconjugates for targeted drug delivery. *J. Controlled Release* **2002**, *78* (1−3), 165–173.

(27) Kopeček, J.; Krinick, N. L. Drug delivery system for the simultaneous delivery of drugs activatable by enzymes and light. U.S. Patent 5,258,453(Nov. 2, 1993).

(28) Krinick, N. L.; Sun, Y.; Joyner, D.; Spikes, J. D.; Straight, R. C.; Kopeček, J. A polymeric drug delivery system for the simultaneous delivery of drugs activatable by enzymes and/or light. *J. Biomater. Sci. Polym. Ed.* **1994**, *5* (4), 303–324.

(29) Peterson, C. M.; Lu, J. M.; Sun, Y.; Peterson, C. A.; Shiah, J. G.; Straight, R. C.; Kopeček, J. Combination chemotherapy and photodynamic therapy with *N*-(2-hydroxypropyl)methacrylamide copolymer-bound anticancer drugs inhibit human ovarian carcinoma heterotransplanted in nude mice. *Cancer Res.* **1996**, *56* (17), 3980–3985.

(30) Shiah, J. G.; Sun, Y.; Peterson, C. M.; Straight, R. C.; Kopeček, J. Antitumor activity of *N*-(2-hydroxypropyl)methacrylamide copolymer-mesochlorin e_6 and adriamycin conjugates in combination treatments. *Clin. Cancer Res.* **2000**, *6* (3), 1008–1015.

(31) Hongrapipat, J.; Kopečková, P.; Prakongpan, S.; Kopeček, J. Enhanced antitumor activity of combinations of free and HPMA copolymer-bound drugs. *Int. J. Pharm.* **2008**, *351*, 259–270.

(32) Fischer, P. M.; Lane, D. P. Small-molecule inhibitors of the p53 suppressor HDM2: have protein-protein interactions come of age as drug targets. *Trends Pharmacol. Sci.* **2004**, *25* (7), 343–346.

(33) Issaeva, N.; Bozko, P.; Enge, M.; Protopopova, M.; Verhoef, L. G.; Masucci, M.; Pramanik, A.; Selivanova, G. Small molecule RITA binds to p53, blocks p53-HDM-2 interaction and activates p53 function in tumors. *Nat. Med.* **2004**, *10* (12), 1321–1328.

(34) Nieves-Neira, W.; Rivera, M. I.; Kohlhagen, G.; Hursey, M. L.; Pourquier, P.; Sausville, E. A.; Pommier, Y. DNA protein cross-links produced by NSC 652287, a novel thiophene derivative active against human renal cancer cells. *Mol. Pharmacol.* **1999**, *56* (3), 478–484.

(35) Rivera, M. I.; Stinson, S. F.; Vistica, D. T.; Jorden, J. L.; Kenney, S.; Sausville, E. A. Selective toxicity of the tricyclic thiophene NSC 652287 in renal carcinoma cell lines: differential accumulation and metabolism. *Biochem. Pharmacol.* **1999**, *57* (11), 1283–1295.

(36) Hopper, C. Photodynamic therapy: a clinical reality in the treatment of cancer. *Lancet Oncol.* **2000**, *1*, 212–219.

(37) Dahl, K. N.; Westhoff, C. M.; Discher, D. E. Fractional attachment of CD47 (IAP) to the erythrocyte cytoskeleton and visual colocalization with Rh protein complexes. *Blood* **2003**, *101* (3), 1194–1199.

(38) Mawby, W. J.; Holmes, C. H.; Anstee, D. J.; Spring, F. A.; Tanner, M. J. Isolation and characterization of CD47 glycoprotein: a multispanning membrane protein which is the same as integrin-associated protein (IAP) and the ovarian tumour marker OA3. *Biochem. J.* **1994**, *304* (Pt 2), 525–530.

(39) Boerman, O.; Massuger, L.; Makkink, K.; Thomas, C.; Kenemans, P.; Poels, L. Comparative in vitro binding characteristics and biodistribution in tumor-bearing athymic mice of anti-ovarian carcinoma monoclonal antibodies. *Anticancer Res.* **1990**, *10* (5A), 1289–1295.

(40) Campbell, I. G.; Freemont, P. S.; Foulkes, W.; Trowsdale, J. An ovarian tumor marker with homology to vaccinia virus contains an IgV-like region and multiple transmembrane domains. *Cancer Res.* **1992**, *52* (19), 5416–5420.

(41) Chou, T. C. Theoretical basis, experimental design, and computerized simulation of synergism and antagonism in drug combination studies. *Pharmacol. Rev.* **2006**, *58* (3), 621–681.

(42) Chou, T. C.; Talalay, P. Quantitative analysis of dose-effect relationships: the combined effects of multiple drugs or enzyme inhibitors. *Adv. Enzyme Regul.* **1984**, *22*, 27–55.

(43) Zhao, L.; Wientjes, M. G.; Au, J. L. Evaluation of combination chemotherapy: integration of nonlinear regression, curve shift, isobologram, and combination index analyses. *Clin. Cancer Res.* **2004**, *10* (23), 7994–8004.

Materials and Methods

Materials. Mce_6 was purchased from Porphyrin Products (Logan, UT). SOS was kindly supplied by the Drug Synthesis and Chemistry Branch, Developmental Therapeutics Program, Division of Cancer Treatment and Diagnosis, National Cancer Institute. All other chemicals were purchased from Sigma Chemical Co. (St. Louis, MO).

Cell Line. The human ovarian carcinoma cell line OVCAR-3 was purchased from American type Culture Collection. Cells were cultured in RPMI 1640 medium (Sigma) containing 10 μg/mL insulin (Sigma) supplemented with 10% fetal bovine serum (HyClone Laboratories, Logan, UT), at 37 °C in a humidified atmosphere of 5% CO_2 (v/v).

OV-TL16 Antibody Production. The OV-TL16 antibody was produced as described previously.[44] Briefly, the OV-TL16 antibody was produced by *in vitro* cartridge bioreactor (Cellulosic-MPS, Spectrum Laboratories, Rancho Dominguez, CA) culture of OV-TL16 hybridoma cells with serum free hybridoma medium (Gibco Life Sciences, Carlsbad, CA). The antibody was purified by applying the supernatant of cell suspension harvested from bioreactor to a protein G Sepharose 4 Fast Flow column (Pharmacia, Piscataway, NJ), equilibrated with binding buffer (0.01 M Na_2HPO_4, 0.15 M NaCl, 0.01 M EDTA pH 7.2). The OV-TL16 antibody was eluted with 0.5 M acetate buffer pH 3.0. The antibody was dialyzed (mol wt cutoff 6−8 kDa) against phosphate buffered saline (PBS) overnight at 4 °C.

Preparation of Fab′ Fragment. The antibody Fab′ fragment was prepared freshly as described previously.[25,44] The OV-TL16 antibody in 0.1 M citric buffer pH 4.0 was digested by 10% (w/w) pepsin (Sigma) for 2.5 h at 37 °C to give $F(ab')_2$. The digestion reaction was monitored by size exclusion chromatography on a Superdex 200 column. The $F(ab')_2$ was reduced to Fab′ with 20 mM cysteine (Sigma) in 20 mM Tris buffer pH 8.5 for 1 h at 37 °C. Excess cysteine was removed on a Sephadex G-25 (PD-10 column, Pharmacia).

Synthesis of Nontargeted HPMA Copolymer−Mce_6 Conjugate (P-GFLG-Mce_6). P-GFLG-Mce_6 was prepared as described previously.[28] Briefly, the conjugate was synthesized using a polymer analogous reaction in two steps. First, the polymer precursor (P-GFLG-ONp) was prepared by radical precipitation copolymerization of HPMA and *N*-methacryloylglycylphenylalanylleucylglycine *p*-nitrophenyl ester (MA-GFLG-ONp).[45,46] Second, Mce_6 was bound to P-GFLG-ONp by aminolysis of reactive ONp groups in *N*,*N*-dimethylformamide (DMF). The reaction solution was precipitated into a mixture of acetone:ether (3:2 (v/v)). The dried precipitate was dissolved in methanol and purified on a Sephadex LH-20 column with methanol/0.5% acetic acid as the elution solvent. The polymer band was collected and evaporated to dryness. The product was dissolved in deionized (DI) water, dialyzed overnight and lyophilized. The product yield was 69%. The structure and characterization of nontargeted polymer conjugates are summarized in Scheme 1A and Table 1.

Synthesis of Nontargeted HPMA Copolymer−SOS Conjugate (P-GFLG-SOS). P-GFLG-SOS (Scheme 1A) was synthesized by binding of SOS to the P-GFLG-ONp polymer precursor via an ester linkage.[31] Briefly, P-GFLG-ONp was dissolved in DMF and mixed with DMF solution of SOS. 4-Dimethylaminopyridine (DMAP) was added, and the reaction was allowed to proceed for 72 h in the dark at room temperature. The product was isolated, after reduction of volume, by precipitation into a mixture of acetone:ether (3:1 (v/v)). The precipitate was dissolved in methanol and applied to a Sephadex LH-20 column with methanol as the mobile phase. The polymer band was collected, concentrated and reprecipitated. The product was a yellowish powder, with a yield of 61%.

Synthesis of HPMA Copolymer−Mce_6 Conjugate Containing Maleimide Groups, P-(GFLG-Mce_6)-MAL. This copolymer precursor was prepared in three steps. The reactions are shown in Scheme 2. First, a polymerizable derivative of Mce_6, *N*-methacryloylglycylphenylalanylleucylglycine Mce_6 (MA-GFLG-Mce_6),[25] was synthesized by reacting MA-GFLG-ONp (60 mg, 0.103 mmol) with Mce_6 (63.5 mg, 0.093 mmol) in DMF (∼2 mL). The reaction solution was stirred at room temperature in the dark for 2 h. *N*,*N*′-diisopropylethylamine (DIPEA; 18 μL, 0.103 mmol) was added and stirring continued overnight. 1-Amino-2-propanol (∼8 μL, 0.103 mmol) and a small amount of *tert*-octylpyrocatechol were added and DMF was removed under reduced pressure. The residue was isolated using a Sephadex LH-20 column with acetone:methanol:acetic acid (2:1:0.1) as the mobile phase. The fractions were collected and checked on TLC. The product fraction was evaporated to dryness, washed with ether, collected by filtration, and dried under vacuum. The molecular weight (M_w) of MA-GFLG-Mce_6 was 1083.6 Da as determined by electrospray ionization mass spectrometry (ESI-MS). The product yield was 90 mg (73%). Second, the polymeric precursor P-(GFLG-Mce_6)-NH_2 was prepared by radical copolymerization of HPMA[47] (107.6 mg, 0.751 mmol), *N*-(3-aminopropyl)methacrylamide hydrochloride (APMA, 16.27 mg, 0.091 mmol; Polysciences, Warrington, PA), and MA-GFLG-Mce_6 (76.9 mg, 0.068 mmol) in methanol (∼1.8 mL) at 50 °C for 48 h, using 2,2′-azobisisobutyronitrile (AIBN; 19.27 mg) as the initiator. The polymerization mixture contained 12.5 wt % of monomers and 1.2 wt % of AIBN. The molar ratio of HPMA:APMA:

(44) Lu, Z. R. Polymerizable Fab′ antibody fragment targeted photodynamic cancer therapy in nude mice. *S.T.P. Pharma Sci.* **2003**, *13* (1), 69–75.

(45) Kopeček, J.; Rejmanová, P.; Strohalm, J.; Ulbrich, K.; Říhová, B.; Chytrý, V.; Lloyd, J.; Duncan, R. Synthetic polymeric drugs. U.S. 5,037,883(Aug. 6, 1991).

(46) Ulbrich, K.; Šubr, V.; Strohalm, J.; Plocová, D.; Jelínková, M.; Říhová, B. Polymeric drugs based on conjugates of synthetic and natural macromolecules. I. Synthesis and physico-chemical characterisation. *J. Controlled Release* **2000**, *64* (1−3), 63–79.

(47) Kopeček, J.; Bažilová, H. Poly[*N*-(2-hydroxypropyl)methacrylamide]. I. Radical polymerization and copolymerization. *Eur. Polym. J.* **1973**, *9* (1), 7–14.

Scheme 1. Chemical Structures of (A) Nontargeted and (B) Fab′-Targeted HPMA Copolymer−Mce_6 or −SOS Conjugates

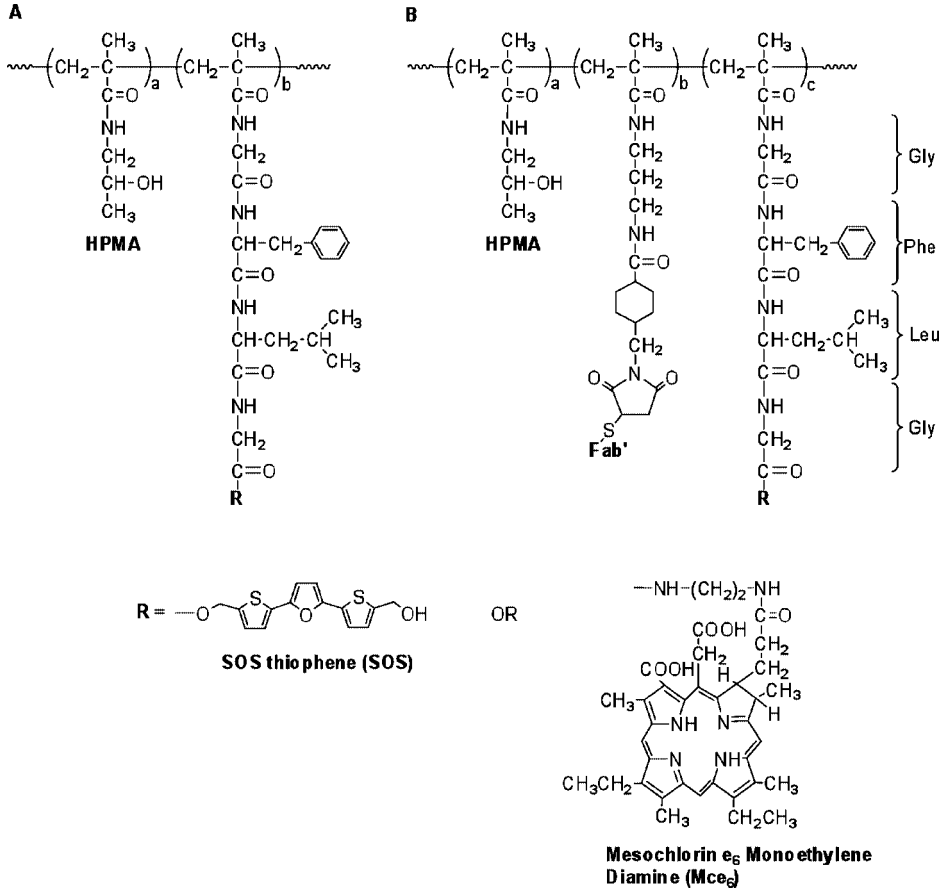

Table 1. Characterization of Nontargeted HPMA Copolymer Conjugates, Polymeric Precursors, and Fluorescently Labeled HPMA Copolymer Conjugates

structures	mol % of side chains[a]	mmol of ligand/ g of polymer conjugate	no. of ligands/ polymer chain (conjugate)	apparent M_w (kDa)[b]
P-GFLG-Mce_6	2.04	0.125	2.9	23
P-GFLG-SOS	1.62	0.106	3.4	32
P-(GFLG-Mce_6)-NH_2	2.62	0.153 (Mce_6)	1.7 (Mce_6)	11
	8.11[c]	0.472 (NH_2)		
P-(GFLG-SOS)-NH_2	4.60	0.270 (SOS)	2.7 (SOS)	10
	4.70[c]	0.272 (NH_2)		
P-(GFLG-Mce_6)-MAL	2.60	0.142 (Mce_6)	2.0 (Mce_6)	14
	6.02[d]	0.329 (MAL)		
P-(GFLG-SOS)-MAL	4.14	0.236 (SOS)	5.2 (SOS)	22
	3.36[d]	0.192 (MAL)		
P-(GFLG-Mce_6)-FITC	*f*	0.060[e]	1.0 (FITC)	*f*
P-(GFLG-SOS)-FITC	*f*	0.038[e]	0.6 (FITC)	*f*
P-(GFLG-Mce_6)-(Fab′-FITC)[g]	*f*	0.063[e]	3.1 (FITC per conjugate)	*f*
P-(GFLG-SOS)-(Fab′-FITC)[g]	*f*	0.050[e]	2.5 (FITC per conjugate)	*f*

[a] Determined by UV spectrophotometry in methanol: $\varepsilon_{395} = 158000\ M^{-1}\ cm^{-1}$ for Mce_6, and $\varepsilon_{358} = 33000\ M^{-1}\ cm^{-1}$ for SOS. [b] Apparent molecular weight (M_w) of polymers was estimated by size exclusion chromatography using AKTA/FPLC (Pharmacia) system equipped with a Superose 6 column, calibrated with polyHPMA fractions. PBS buffer pH 7.3 + 30% (v) acetonitrile and 0.1 M acetate buffer pH 5.5 + 30% (v) acetonitrile were used for polymer conjugates containing Mce_6 and polymer conjugates containing SOS, respectively. [c] Determined by ninhydrin assay. [d] Determined by 5-((2-(and-3)-*S*-(acetylmercapto)succinoyl)amino)fluorescein assay (SAMSA assay, Molecular Probes). [e] Determined by spectrophotometric determination of FITC ($\varepsilon_{497} = 73\ 000\ M^{-1}\ cm^{-1}$ in 0.1 M sodium borate buffer). [f] Not determined. [g] Fluorescently labeled targeted conjugates were prepared by reacting P-(GFLG-Mce_6)-Fab′ and P- (GFLG-SOS)-Fab′ (Table *2*) with 5-SFX.

MA-GFLG-Mce_6 was 82.5:10:7.5. The reaction mixture was purified on a Sephadex LH-20 column eluted with methanol. The polymer fraction was collected, and methanol was evaporated. The residue was precipitated in a mixture of acetone:ether (1:2 (v/v)). The precipitate was dissolved in water, dialyzed (mol wt cutoff 6−8 kDa) against DI water

Table 2. Characterization of Fab′-Targeted HPMA Copolymer−Mce_6/−SOS Immunoconjugates

structures	wt % drug:polymer:Fab′[a]	molecular ratio drug:polymer:Fab′	mol wt (kDa)[b]
P-(GFLG-Mce_6)-Fab′	2.1:21.1:76.8	2:1:1	64
P-(GFLG-SOS)-Fab′	1.6:23.5:74.9	5:1:1	72

[a] Mce_6 and SOS contents determined by UV spectrophotometry in methanol: $\varepsilon_{395} = 158000\ M^{-1}\ cm^{-1}$ for Mce_6, $\varepsilon_{358} = 33000\ M^{-1}\ cm^{-1}$ for SOS. Protein content was determined by Lowry assay. [b] Calculated from the composition of polymer (molecular ratio of drug, polymer, and Fab′).

and lyophilized. The product yield was 65 mg (32%). Third, polymeric precursor P-(GFLG-Mce_6)-MAL was prepared by reacting P-(GFLG-Mce_6)-NH_2 (55 mg, 0.026 mmol NH_2 group) with succinimidyl *trans*-4-(maleimidomethyl)cyclohexane-1-carboxylate (SMCC; 17.36 mg, 0.052 mmol) (Soltec Ventures, Beverly, MA) and DIPEA (∼13 μL, 0.078 mmol). The mole ratio of NH_2:SMCC:DIPEA was 1:2:3. P-(GFLG-Mce_6)-NH_2 was dissolved in 0.3 mL of DMF and SMCC in 0.9 mL of DMF. The polymer solution was added into the SMCC solution. DIPEA was added dropwise. The reaction solution was stirred overnight at room temperature. DMF was removed under reduced pressure to dryness. The residue was dissolved in a small volume of methanol and purified on a Sephadex LH-20 column eluted with a mixture of methanol and 0.1% acetic acid. The copolymer band was collected, evaporated and precipitated into a mixture of acetone:ether (1:1). The characterization of copolymer precursors is shown in Table 1.

Synthesis of HPMA Copolymer−SOS Conjugate Containing Maleimide Groups, P-(GFLG-SOS)-MAL. This copolymer precursor was also prepared by three-step reaction. The procedure is shown in Scheme 2. First, MA-GFLG-ONp (278.6 mg, 0.480 mmol) and SOS (200 mg, 0.680 mmol) were dissolved in tetrahydrofuran (THF; ∼15 mL). DMAP (44.6 mg, 0.370 mmol) was added. The reaction mixture was stirred at room temperature in the dark for 72 h. The mixture was concentrated under reduced pressure. The residue was isolated using silica gel column chromatography. The excess free drug was recovered by elution with acetone:hexane (2:1), and the fractions were collected by eluting with acetone and then with methanol. The fractions were checked on TLC. The product-containing fraction was evaporated and recrystallized with THF/hexane. The M_w of MA-GFLG-SOS was 734.2 Da as determined by ESI-MS. The product yield was 130 mg (27%). Second, polymeric precursor, P-(GFLG-SOS)-NH_2, was synthesized by copolymerization of HPMA (141.3 mg, 0.987 mmol), APMA (14.2 mg, 0.079 mmol), and MA-GFLG-SOS (50 mg, 0.068 mmol) in DMF (1 mL) and acetone (0.5 mL) at 50 °C for 48 h, using AIBN (19.7 mg) as the initiator. The molar ratio of HPMA:APMA:MA-GFLG-SOS was 87:7:6. The reaction mixture was purified on a Sephadex LH-20 column eluted with methanol. The polymer fraction was collected and evaporated to the viscous residue. The residue was precipitated into acetone:ether (1:1). The product yield was 150 mg (73%). Third, polymeric precursor P-(GFLG-SOS)-MAL was prepared by using the same procedure as for P-(GFLG-Mce_6)-MAL. P-(GFLG-SOS)-NH_2 (145 mg, 0.040 mmol NH_2 groups) and SMCC (26.41 mg, 0.079 mmol) were dissolved separately in DMF (∼2.5 mL and ∼0.5 mL, respectively). DIPEA (∼21 μL, 0.119 mmol) was used. The product was applied on a Sephadex LH-20 column and eluted with methanol without acetic acid. The product was precipitated and filtered off, with a yield of 130 mg (76%). The characterization of conjugates is shown in Table 1.

Preparation of Antibody Fab′ Fragment-Targeted HPMA Copolymer−Mce_6/−SOS Conjugates, P-(GFLG-Mce_6)-Fab′ and P-(GFLG-SOS)-Fab′. The targeted conjugates were prepared by dissolving P-(GFLG-Mce_6)-MAL or P-(GFLG-SOS)-MAL precursor in 20 mM MES buffer pH 6.5 and reacting with freshly prepared Fab′ fragment (polymer:Fab′ weight ratio = 1:2) overnight in the dark at 4 °C. The product was purified on a DEAE Sepharose Fast Flow ion exchange column (Pharmacia), eluted using 20 mM Bis-Tris buffer pH 6.5 with a gradient NaCl concentration of 0−0.5 M. The fraction corresponding to conjugate was confirmed by size exclusion chromatography using Superose 6 (HR 10/30) column. The structure and composition of polymer conjugates are summarized in Scheme 1B and Table 2.

Preparation of Fluorescein-Labeled Nontargeted HPMA Copolymer−Mce_6/−SOS Conjugates, P-(GFLG-Mce_6)-FITC and P-(GFLG-SOS)-FITC. 6-(Fluorescein-5-carboxamido)hexanoic acid succinimidyl ester (5-SFX; ∼0.1 mg, 0.170 μmol) was dissolved in dimethylsulfoxide (25 μL) and DI water (100 μL). The polymer precursor P-(GFLG-Mce_6)-NH_2 or P-(GFLG-SOS)-NH_2 (∼3 mg, ∼1 μmol of NH_2) was dissolved in DI water (∼300 μL). The 5-SFX solution was added into the polymer solution. DIPEA (∼1 drop) was added into the reaction solution while stirring. The mixture was stirred at room temperature in the dark for 1 h. Saturated Na_2HPO_4 (∼20 μL) was added to stop the reaction. The product was separated on a PD-10 column and eluted with PBS.

Preparation of Fluorescein-Labeled Fab′-Targeted HPMA Copolymer−Mce_6/−SOS Conjugates, P-(GFLG-Mce_6)-(Fab′-FITC) and P-(GFLG-SOS)-(Fab′-FITC). P-(GFLG-Mce_6)-Fab′ and P-(GFLG-SOS)-Fab′ were reacted with 5-SFX. The procedure was as described for P-(GFLG-Mce_6)-FITC and P-(GFLG-SOS)-FITC. The characterization of fluorescently labeled copolymer conjugates is shown in Table 1.

Drug Stock Solution Preparations. SOS was dissolved in PBS containing cyclodextrin (5% (w/v) cyclodextrin in PBS/1 mg of SOS) to enhance the solubility of SOS.[48] P-GFLG-SOS, P-(GFLG-Mce_6)-Fab′, and P-(GFLG-SOS)-Fab′ were prepared in PBS. Other samples (Mce_6 and P-GFLG-Mce_6) were prepared in DI water. All stock

(48) Alley, M. C.; Hollingshead, M. G.; Dykes, D. J.; Waud, W. R. Human tumor xenograft models in NCI drug development. In *Anticancer Drug Development Guide: Preclinical Screening, Clinical Trials, and Approval*, 2nd ed.; Teicher, B. A., Andrews, P. A, Eds.; Humana Press: Totowa, NJ, 2004; pp 125−152.

Scheme 2. Synthesis and Chemical Structure of HPMA Copolymer−Mce_6/−SOS Conjugates Containing Maleimide Group [P-(GFLG-Mce_6)-MAL and P-(GFLG-SOS)-MAL, Respectively]

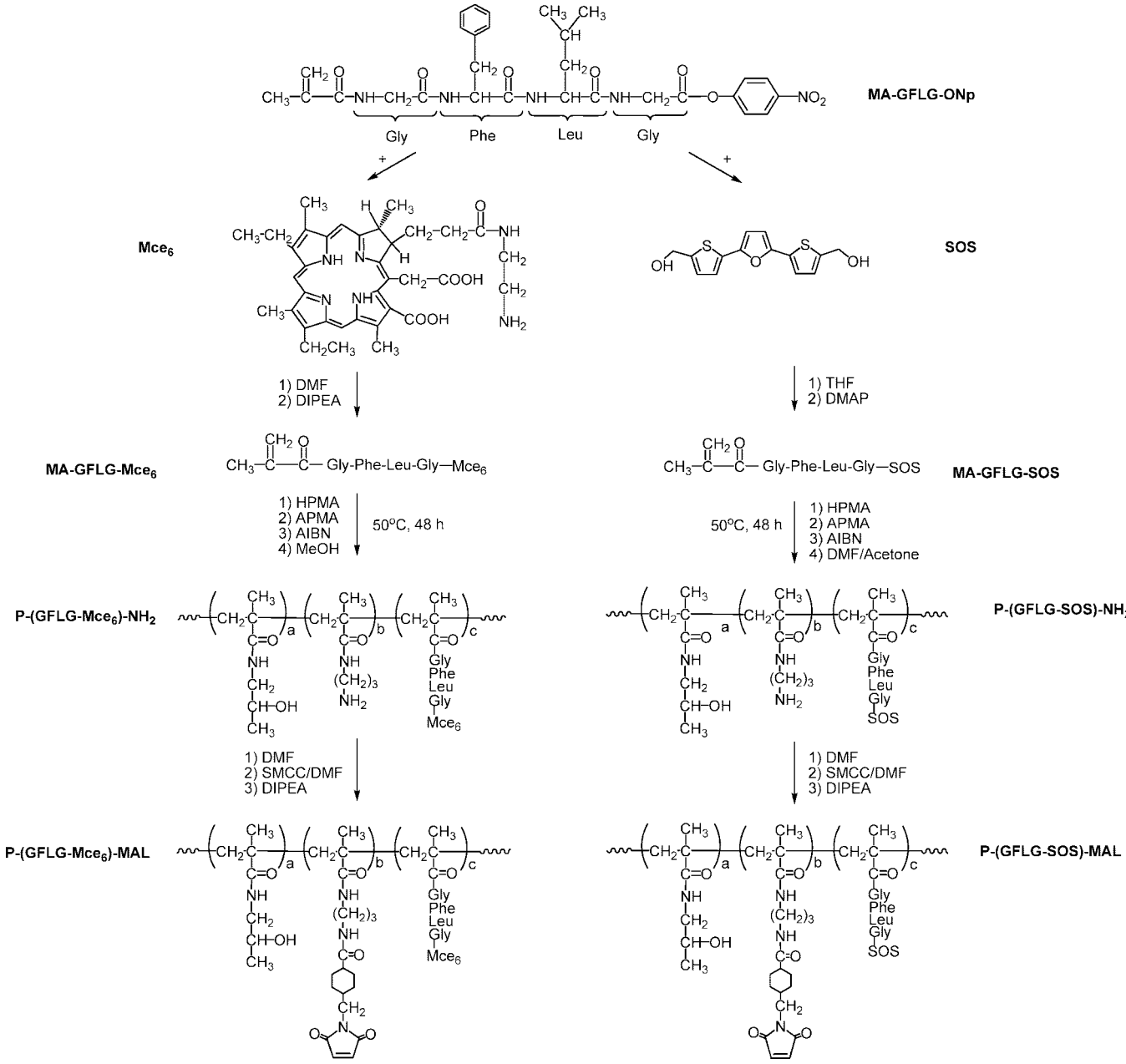

solutions were sterile-filtered. Drug contents were determined by UV spectrophotometry. All stock solutions were freshly prepared and gradually diluted with RPMI 1640 culture medium before use.

Confocal Microscopy. Fifty thousand OVCAR-3 cells were subcultured into an eight-chamber slide and incubated for 2 days at 37 °C in a humidified atmosphere of 5% CO_2. The cells in each chamber were exposed to fluorescein-labeled copolymer conjugates (at 20 μM FITC equivalent) at 37 °C for 1 h in the dark. Cells were fixed with 2% paraformaldehyde for 20 min at room temperature and washed twice with PBS. The chamber slide was covered with a cover slide utilizing antifade reagent (Molecular Probes). The cell internalization of fluorescently labeled HPMA copolymer conjugates was imaged using a Zeiss (Thornwood, NY) LSM 510 confocal imaging system.

Flow Cytometry. OVCAR-3 cells (75,000 cells/well) were seeded into a 24-well plate and incubated for 24 h at 37 °C in a humidified atmosphere of 5% CO_2. Cells in each well were exposed to the fluorescein-labeled copolymer conjugates (at 20 μM FITC equivalent) at 37 °C for 1 h in the dark. The medium was removed. The cell monolayer was rinsed twice with ice-cold PBS and detached from the well surface by incubation with TrypLE Express (Gibco) for 2 min. All steps were carried out on ice to minimize efflux of the sample. The cells were suspended with ice-cold PBS containing 0.2% FBS, maintained in suspension on ice in the dark and processed for flow cytometry utilizing FACScan

Scheme 3. Experimental Protocols Used in the Cytotoxicity Study

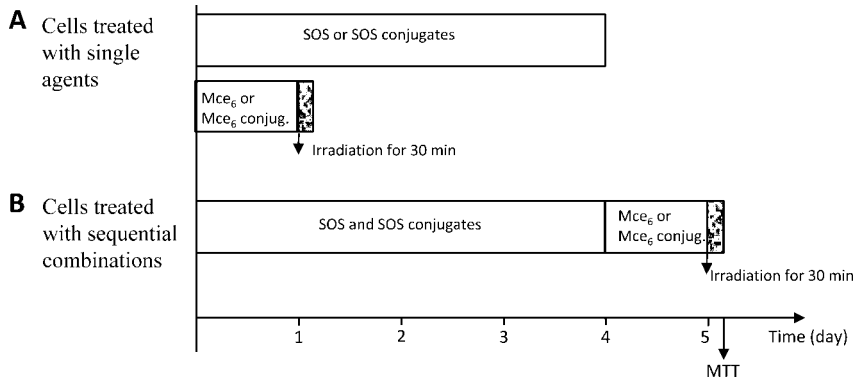

instrument (Becton Dickinson). Twenty thousand events were collected per sample. Control cells were not exposed to the sample to assess the endogenous fluorescence of the cells.

Additional experiments were performed at 0 °C (on ice) to demonstrate the surface binding of targeted conjugates. OVCAR-3 cells, growth medium and the fluorescein-labeled conjugates (at 10 μM FITC equivalent) were precooled on ice before experiments. The cells were exposed to conjugates for 2 h, then the medium containing conjugates was discarded, and cells were washed extensively with cold PBS and processed for flow cytometry as described above.

Cytotoxicity Bioassays. The drug concentration that inhibited cell growth by 50% compared with control cells (IC_{50}) was determined using a modified 3-(4,5-dimethylthiazol-2-yl)-2,5-diphenyltetrazolium bromide (MTT) assay.[49] Cells were seeded in 96-well flat bottom microplates at a density of 10,000 cells/well in 200 μL of RPMI 1640 medium and allowed to grow for ~30 h. The cells were then exposed to various concentrations of each free drug alone (Mce$_6$ and SOS), each nontargeted copolymer conjugate (P-GFLG-Mce$_6$ and P-GFLG-SOS), each targeted copolymer conjugate [P-(GFLG-Mce$_6$)-Fab′ and P-(GFLG-SOS)-Fab′], or their sequential combinations ($n = 6$ in single experiment). The different treatment protocols are shown in Scheme 3. During the cells' exposure to drug(s), they were incubated at 37 °C in a humidified atmosphere of 5% CO_2 and in the dark condition. After 4 days of exposure for SOS and its conjugates or 1 day of exposure for Mce$_6$ and its conjugates, the drugs were removed, cells were washed with warm PBS and the medium (300 μL) was replaced. For cell growth inhibition studies using Mce$_6$, P-GFLG-Mce$_6$, or P-(GFLG-Mce$_6$)-Fab′ (alone or in combinations), the cells were irradiated with three tungsten halogen lamps through a 650 nm band-pass filter at 3.0 mW/cm^2 for 30 min. After an additional 1 day or 4 days in culture for SOS and its conjugates or for Mce$_6$ and its conjugates, respectively, medium was removed and replaced with 100 μL of fresh medium and 10 μL of sterile-filtered MTT solution (5 mg/mL in PBS). After incubating for 24 h, 150 μL of 20% (w/v) sodium dodecyl sulfate in water was added to each well and incubated overnight. The following day, the absorbance of each well was read at 570 nm with a reference wavelength at 630 nm. Untreated cells served as a 100% cell viability control, and the media served as background reference. Growth inhibition was expressed as the growth of drug-treated cells related to that of untreated control cells.

Determination of Drug Interaction and Combination Index. In combination treatment studies, OVCAR-3 cells were treated with a dose range of SOS for 4 days followed by a dose range of Mce$_6$ for 1 day, and irradiated for 30 min ($n = 6$ in single experiment), as shown in Scheme 3. After each step the drug was removed and the cells were washed with warm PBS. Drug interaction and CI were determined using median-effect analysis according to the method of Chou and Talalay.[41,42] The median-effect equation describes dose−effect relationships, which is expressed by $f_a/f_u = (D/D_m)^m$ or $\log(f_a/f_u) = m \log(D) - m \log(D_m)$ where f_a and f_u are the fraction affected [1 − (absorbance of treatment well − average of absorbance of blanks)/(average of absorbance of untreated cell wells − average of absorbance of blanks)] and unaffected ($f_u = 1 - f_a$) by the dose or concentration D, D_m is the median-effect dose (IC_{50}) that inhibits the cell growth by 50%, and m is the coefficient signifying the shape of the dose−effect relationship. Based on the logarithmic conversion, the plot of $x = \log(D)$ versus $y = \log(f_a/f_u)$ is called the median-effect plot and D_m is calculated from the antilog of the x-intercept. The CI describes the interaction between two drugs and quantitates the synergism, antagonism or additive effects. The CI is determined by the equation $CI = [(D)_1/(D_x)_1] + [(D)_2/(D_x)_2]$ where $(D_x)_1$ and $(D_x)_2$ are the doses of drug 1 alone and drug 2 alone that inhibit the cell growth x%, respectively. $(D)_1$ and $(D)_2$ are for doses in combination that also inhibit x%. The CI values were calculated for different values of f_a and plotting the CI values as a function of f_a values, using CompuSyn software (ComboSyn Inc., Paramus, NJ). In the f_a−CI plot, CI < 1, = 1, and > 1 indicate synergism, additivity, and antagonism, respectively.

Statistical Analysis. All mean values are presented as means ± standard deviation ($n = 6$ in a single experiment).

(49) Hansen, M. B.; Nielsen, S. E.; Berg, K. Re-examination and further development of a precise and rapid dye method for measuring cell growth/cell kill. *J. Immunol. Methods* **1989**, *119* (2), 203–210.

Results and Discussion

Characteristics of HPMA Copolymer−Mce_6/−SOS Conjugates. The structures of HPMA copolymer conjugates, P-GFLG-Mce_6, P-GFLG-SOS, P-(GFLG-Mce_6)-Fab′, and P-(GFLG-SOS)-Fab′, are shown in Scheme 1. The drugs, Mce_6 and SOS, were bound to the HPMA copolymer backbone via a GFLG spacer, stable in the bloodstream, but susceptible to enzymatically catalyzed hydrolysis in the lysosomal compartment of the cells.[50−52] For Fab′ attachment, the amino groups of APMA monomer units in HPMA copolymer precursors were first converted to maleimido groups by reaction with a heterobifunctional agent, SMCC (Scheme 2), followed by attachment of Fab′ via thioether bonds. For some experiments, fluorescently labeled conjugates were synthesized. In nontargeted conjugates, the 5-SFX was attached to amino groups of APMA monomer units. The Fab′-targeted conjugates were labeled by the reaction of 5-SFX with the final conjugates.

The characteristics of HPMA copolymer precursors, nontargeted HPMA copolymer conjugates, Fab′-targeted HPMA copolymer conjugates, and fluorescently labeled conjugates are summarized in Tables 1 and 2. P-GFLG-Mce_6, P-GFLG-SOS, P-(GFLG-Mce_6)-Fab′, and P-(GFLG-SOS)-Fab′ conjugates contained 2.9, 3.4, 2.0, and 5.0 drug molecules per macromolecule, respectively. P-(GFLG-Mce_6)-Fab′ and P-(GFLG-SOS)-Fab′ had drug:polymer:Fab′ molecular ratios of approximately 2:1:1 and 5:1:1, respectively. The M_w of Fab′-targeted copolymer conjugates were 2.2 to 2.8 times higher than those of nontargeted conjugates.

Intracellular Uptake of Fluorescein-Labeled Fab′-Targeted HPMA Copolymer Conjugates. Unlike low molecular weight drugs that enter cells by diffusion through the plasma membrane, macromolecules are internalized within membrane-limited vesicles in the process of endocytosis. Several basic internalization mechanisms, clathrin-mediated endocytosis, caveolae-mediated endocytosis, clathrin- and caveolin-independent endocytosis, and macropinocytosis have been identified.[53,54] To a greater or lesser extent, two or more distinct mechanisms coexist when a single cell type internalizes macromolecule−drug conjugates.[55]

Studies on the subcellular fate of HPMA copolymer−drug conjugates demonstrated that the conjugates are lysosomotropic and will accumulate in the lysosomal compartment of the cell. Tijerina et al., using subcellular fractionation, determined the localization of a considerable fraction of HPMA copolymer−Mce_6 conjugates in the lysosomal compartment of human ovarian carcinoma A2780 cells.[56] Omelyanenko et al. used pH dependent fluorescence of FITC to display the lysosomotropism of FITC-labeled HPMA copolymers containing *N*-acylated galactosamine in HepG2 hepatocarcinoma cells.[57]

Recently, the uptake mechanism of HPMA copolymer−DOX conjugate in human ovarian carcinoma OVCAR-3 cells was studied by confocal fluorescence microscopy and by colocalization experiments with substrates specific for a particular internalization mechanism. The results suggested that the HPMA copolymer−DOX conjugate is internalized via both clathrin- and caveolae-mediated endocytosis.[55]

The biorecognition and cellular uptake of P-(GFLG-Mce_6)-(Fab′-FITC) and P-(GFLG-SOS)-(Fab′-FITC) was studied using confocal microscopy (Figure 1) and flow cytometry (Figures 2 and 3). Nontargeted conjugates, P-(GFLG-Mce_6)-FITC and P-(GFLG-SOS)-FITC, served as controls. After a 1 h exposure of OVCAR-3 cells to HPMA copolymer conjugates at 37 °C, the intracellular concentrations of targeted polymer conjugates containing Mce_6 and SOS were significantly higher when compared to nontargeted conjugates. Both confocal microscopy images and flow cytometry profiles displayed very similar results.

However, at 37 °C two processes, biorecognition at surface and internalization by endocytosis, are operative. To clearly demonstrate the biorecognition of targeted conjugates by the CD47 antigen, OVCAR-3 cells were exposed to conjugates at 0 °C. Flow cytometry data at 0 °C, at conditions that suppress endocytosis, demonstrated the biorecognition of P-(GFLG-Mce_6)-Fab′ and P-(GFLG-SOS)-Fab′ conjugates by OVCAR-3 cells (Figure 3). After incubation of OVCAR-3 cells with targeted and nontargeted conjugates for 2 h, no increase in fluorescent intensity (when compared to controls not exposed to any conjugates) in cells incubated with P-GFLG-Mce_6 and P-GFLG-SOS was observed. In contrast, higher fluorescent intensities were detected in cells incubated with targeted (Fab′ containing) conjugates P-(GFLG-Mce_6)-Fab′ and P-(GFLG-SOS)-Fab′. Presumably, the fluorescent signals were derived from membrane associated conjugates as a result of Fab′−CD47 interactions.

These results indicated the biorecognition of HPMA copolymer conjugates containing the Fab′ antibody fragment by OVCAR-3 cells. The results of confocal microscopy are

(50) Kopeček, J. Controlled biodegradability of polymers—a key to drug delivery systems. *Biomaterials* **1984**, *5* (1), 19–25.
(51) Kopeček, J.; Rejmanová, P. Enzymatically Degradable Bonds in Synthetic Polymers. In *Controlled Drug Delivery*; Bruck, S. D., Ed.; CRC Press: Boca Raton, FL, 1983; pp 81−124.
(52) Rejmanová, P.; Pohl, J; Baudyš, M.; Kostka, V.; Kopeček, J. Polymers containing enzymatically degradable bonds. 8. Degradation of oligopeptide sequences in *N*-(2-hydroxypropyl)methacrylamide copolymers by bovine spleen cathepsin B. *Makromol. Chem.* **1983**, *184* (10), 2009–2020.
(53) Roth, M. G. Clathrin-mediated endocytosis before fluorescent proteins. *Nat. Rev. Mol. Cell Biol.* **2006**, *7* (1), 63–68.
(54) Soldati, T.; Schliwa, M. Powering membrane traffic in endocytosis and recycling. *Nat. Rev. Mol. Cell Biol.* **2006**, *7* (12), 897–908.
(55) Liu, J.; Pan, H.; Kopečková, P.; Kopeček, J. Internalization and Subcellular Fate of HPMA Copolymer−Doxorubicin Conjugates; International Symposium on Polymer Therapeutics ISPT-07, Berlin, Germany, February 19−21, 2007; Proceedings, p 49.
(56) Tijerina, M.; Kopečková, P.; Kopeček, J. Correlation of subcellular compartmentalization of HPMA copolymer-Mce_6 conjugates with therapeutic activity in human ovarian carcinoma cells. *Pharm. Res.* **2003**, *20*, 728–737.
(57) Omelyanenko, V.; Kopečková, P.; Gentry, C.; Kopeček, J. Targetable HPMA copolymer-adriamycin conjugates. Recognition, internalization, and subcellular fate. *J. Controlled Release* **1998**, *53* (1−3), 25–37.

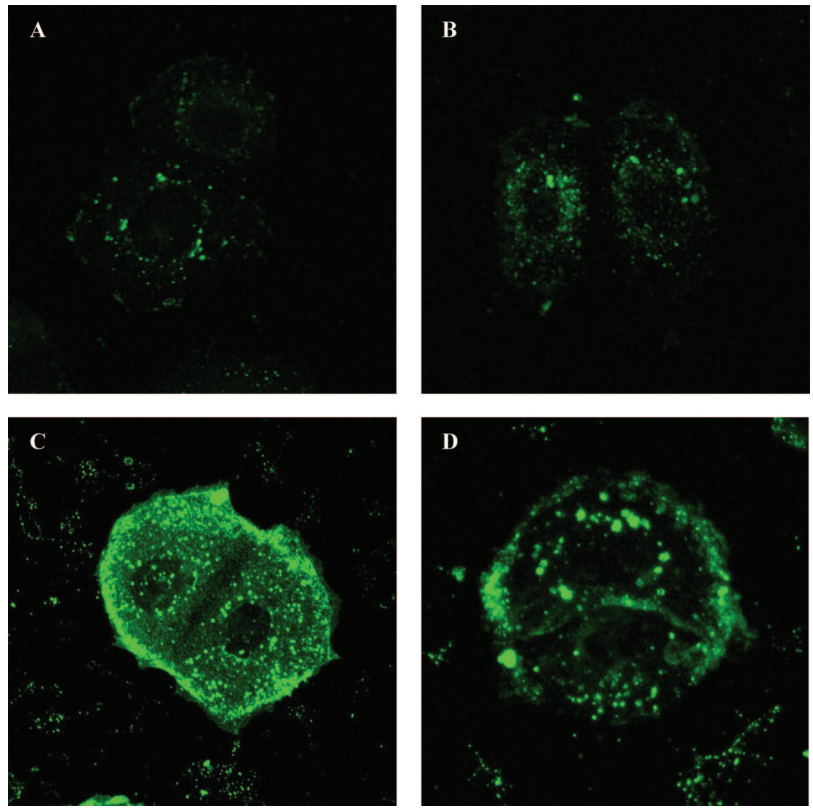

Figure 1. Confocal image of fixed OVCAR-3 cells incubated with fluorescein-labeled HPMA copolymer conjugates in RPMI 1640 culture medium for 1 h in the dark. (A) P-(GFLG-Mce$_6$)-FITC, (B) P-(GFLG-SOS)-FITC, (C) P-(GFLG-Mce$_6$)-(Fab′-FITC), and (D) P-(GFLG-SOS)-(Fab′-FITC).

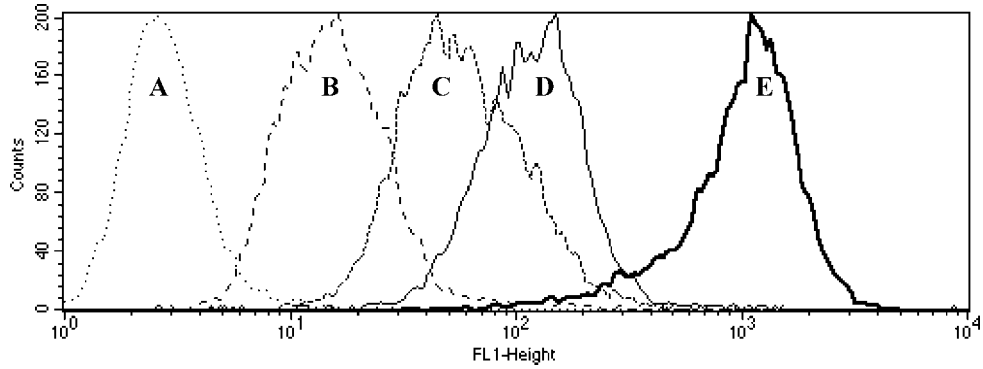

Figure 2. Flow cytometry profiles of OVCAR-3 cells incubated with fluorescein-labeled HPMA copolymer conjugates in RPMI 1640 culture medium for 1 h in the dark. (A) Control cells, (B) P-(GFLG-Mce$_6$)-FITC, (C) P-(GFLG-SOS)-FITC, (D) P-(GFLG-SOS)-(Fab′-FITC), (E) P-(GFLG-Mce$_6$)-(Fab′-FITC).

consistent with the internalization of targeted HPMA copolymer conjugates via receptor-mediated endocytosis, and of the nontargeted conjugates, containing hydrophobic drugs, by fluid-phase pinocytosis and adsorptive pinocytosis, concurrently.

The data are consistent with our previous results on the determination of binding constants of OV-TL16 antibody targeted HPMA copolymers toward OVCAR-3 cells.[58] The affinity constant, K_a, of free antibody was 8×10^{-8} M^{-1}, whereas the K_a for the P-(GG-Mce$_6$)-Fab′ was 3×10^{-8} M^{-1}. The minor decrease in the affinity may be a result of chemical modification and/or steric hindrance of the polymer chain upon the formation of the antibody−antigen complex.

In Vitro **Inhibition of OVCAR-3 Cell Growth by Drugs as Single Agents.** The growth inhibitory effects of Mce$_6$, SOS, P-GFLG-Mce$_6$, P-GFLG-SOS, P-(GFLG-Mce$_6$)-Fab′, and P-(GFLG-SOS)-Fab′ as single agents on OVCAR-3 cells were evaluated after drug exposure using the MTT assay. The IC_{50} values for the free drugs, nontargeted and targeted HPMA copolymer conjugates are shown in Table 3. The 1-day Mce$_6$ exposure and 4-day SOS exposure have been selected based on preliminary experiments on the relationship between exposure time and cell inhibition effect (data not shown). After 1-day Mce$_6$ exposure and 4-day SOS exposure, the cells were more susceptible to Mce$_6$ than SOS about 2 times. It is

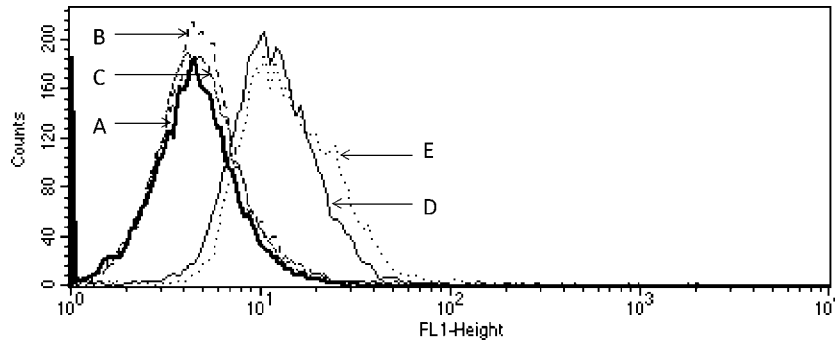

Figure 3. Flow cytometry profiles of OVCAR-3 cells incubated with fluorescein-labeled HPMA copolymer conjugates in RPMI 1640 culture medium for 2 h in the dark at 0 °C. (A) Control cells, (B) P-(GFLG-Mce_6)-FITC, (C) P-(GFLG-SOS)-FITC, (D) P-(GFLG-SOS)-(Fab′-FITC), (E) P-(GFLG-Mce_6)-(Fab′-FITC).

Table 3. IC_{50} Values for Mce_6, SOS, and HPMA Copolymer−Mce_6/−SOS Conjugates against OVCAR-3 Cells

drug	incubation time (days)	IC_{50} or D_m (μM)[a]
Mce_6	1	3.34 ± 0.43
P-GFLG-Mce_6	1	12.5 ± 1.06
P-(GFLG-Mce_6)-Fab′	1	1.35 ± 0.10
SOS	4	2.02 ± 0.17
P-GFLG-SOS	4	32.9 ± 4.94
P-(GFLG-SOS)-Fab′	4	43.8 ± 2.90

[a] D_m is the median-effect dose that inhibits the cell growth by 50%. IC_{50} and D_m values are the means ± SEM (n = 6 in single experiment).

interesting to note the enormous difference in the activity of SOS toward OVCAR-3 cells and toward the human A498 renal cell line.[31] Our previous study on human renal A498 cells demonstrated that free SOS and P-GFLG-SOS conjugates were effective individually and in combination with free DOX and P-GFLG-DOX or free Mce_6 and P-GFLG- Mce_6, respectively.[31] The IC_{50} values for Mce_6 toward both cell types (OVCAR-3 and A498[31]) were similar. However, SOS was very effective toward A498 cells (IC_{50} = 3 nM),[31] but its activity toward OVCAR-3 was about 670 times lower. These data are consistent with the results of the NCI anticancer drug screen consisting of a panel of 60 human cancer cell lines. Rivera et al. showed that after a 2-day continuous exposure to SOS, OVCAR-3 cells were less sensitive to SOS than the A498 cells.[35] These results reflect the different p53 status in these cell lines. The inhibitory effect of SOS is mediated through p53; the disruption of the p53-HDM-2 interactions results in increasing p53 accumulation in tumor cells.[33] It was demonstrated that the p53 status of A498 cells and OVCAR-3 cells is wild-type and mutant, respectively.[59] However, the study of the p53 gene in human ovarian carcinoma cell lines by Yaginuma and Westphal showed that the wild-type p53 protein was detectable in OVCAR-3 cells by immunoprecipitation analysis.[60] These reports indicated that OVCAR-3 cells can be inhibited by higher concentrations of SOS, but have a considerably lower sensitivity when compared to the A498 cell line.

The IC_{50} doses of nontargeted conjugates, P-GFLG-Mce_6 and P-GFLG-SOS, were higher than those of free Mce_6 and SOS, respectively. These results reflect the different mechanisms of cell entry of free drugs vs copolymer conjugates.[61] In contrast, the targeted P-(GFLG-Mce_6)-Fab′ conjugate was 2 and 9 times more effective than Mce_6 and P-GFLG-Mce_6, respectively. The cytotoxicity data with Mce_6 conjugates were in agreement with biorecognition data and internalization mechanisms (Figures 1, 2 and 3). There was a discrepancy in data obtained for P-(GFLG-SOS)-Fab′. This conjugate showed faster internalization (Figure 1) and moderately better biorecognition (Figure 2) than P-GFLG-SOS; however, it possessed a slightly weaker inhibitory effect than P-GFLG-SOS (Table 3). One explanation may be in the long drug exposure time. After long exposure times the intracellular drug content of targeted and nontargeted conjugates may be similar.[62] Furthermore, the efficacies of SOS and its conjugates might be limited by the problem of SOS trafficking to the subcellular compartments where p53 is

(58) Omelyanenko, V.; Kopečková, P.; Gentry, C.; Shiah, J. G.; Kopeček, J. HPMA copolymer-anticancer drug-OV-TL16 antibody conjugates. 1. Influence of the method of synthesis on the binding affinity to OVCAR-3 ovarian carcinoma cells in vitro. *J. Drug Targeting* **1996**, *3* (5), 357–373.

(59) O'Connor, P. M.; Jackman, J.; Bae, I.; Myers, T. G.; Fan, S.; Mutoh, M.; Scudiero, D. A.; Monks, A.; Sausville, E. A.; Weinstein, J. N.; Friend, S.; Fornace, A. J., Jr.; Kohn, K. W. Characterization of the p53 tumor suppressor pathway in cell lines of the National Cancer Institute anticancer drug screen and correlations with the growth-inhibitory potency of 123 anticancer agents. *Cancer Res.* **1997**, *57* (19), 4285–4300.

(60) Yaginuma, Y.; Westphal, H. Abnormal structure and expression of the p53 gene in human ovarian carcinoma cell lines. *Cancer Res.* **1992**, *52* (15), 4196–4199.

(61) Duncan, R.; Rejmanová, P.; Kopeček, J.; Lloyd, J. B. Pinocytic uptake and intracellular degradation of *N*-(2-hydroxypropyl)-methacrylamide copolymers. A potential drug delivery system. *Biochim. Biophys. Acta* **1981**, *678* (1), 143–150.

(62) Marecos, E.; Weissleder, R.; Bogdanov, A., Jr. Antibody-mediated versus nontargeted delivery in a human small cell lung carcinoma model. *Bioconjugate Chem.* **1998**, *9* (2), 184–191.

mainly located, such as nucleus and mitochondria.[63] Subcellular targeting is very important for some active agents and macromolecular therapeutics that have to be transported to their assigned cell organelles. Once those molecules are delivered to the cytosol, various approaches to locate drugs in a particular subcellular organelle have been performed, such as the use of nuclear localization peptides,[56,64] cell-penetrating peptides,[65] lipophilic cationic moieties,[2] and mitochondrial localization agents.[66]

The OA-3 surface antigen (CD47 or IAP) was chosen as delivery target in this study because it is overexpressed in about 90% of the ovarian tumors and only weakly expressed in normal tissue.[39] A panel of anti-CD47 mAbs used in the study of Mawby et al., such as NBTS/BRIC-125 (BRIC-125), NBTS/BRIC-126 (BRIC-126) and NBTS/BRIC-154 (BRIC-154), showed an extremely broad tissue distribution, not only in ovarian carcinomas studied, but also in all hematopoietic cells, mesenchyme and epithelia at multiple sites.[38] On the contrary, the tissue distribution of ^{125}I-labeled OV-TL16 mAb in OVCAR-3 bearing nude mice 48 h after iv injection studied by Boerman et al. demonstrated that ^{125}I-labeled OV-TL16 mAb possessed tumor/nontumor ratio of about 3−15.[39] Furthermore, the mAb OV-TL3 used by Campbell et al. to define OA3 showed little or no reactivity with normal tissues but reacted with most ovarian carcinomas.[40] Slobbe et al. studied the structure of OV-TL3 and OV-TL16 antibodies and reported that both mAbs are able to bind to same epitopic regions on the ovarian carcinoma membrane antigen OA3, although structurally different in their VH regions.[67]

The basis for the difference between mAbs used in the study of Mawby et al. and Boerman et al. or Campbell et al. is unknown and deserves further investigation. One possibility is that an unusual amino acid sequence in the OA3 isoforms is expressed in ovarian cancer cells, and that OV-TL3 and OV-TL16 recognize epitopes in this sequence.[38]

(63) Shmueli, A.; Oren, M. Regulation of p53 by Mdm2: fate is in the numbers. *Mol. Cell* **2004**, *13* (1), 4–5.

(64) Tijerina, M.; Kopečková, P.; Kopeček, J. Mechanisms of cytotoxicity in human ovarian carcinoma cells exposed to free Mce_6 or HPMA copolymer-Mce_6 conjugates. *Photochem. Photobiol.* **2003**, *77* (6), 645–652.

(65) Nori, A.; Jensen, K. D.; Tijerina, M.; Kopečková, P.; Kopeček, J. Tat-conjugated synthetic macromolecules facilitate cytoplasmic drug delivery to human ovarian carcinoma cells. *Bioconjugate Chem.* **2003**, *14* (1), 44–50.

(66) Callahan, J.; Kopeček, J. Semitelechelic HPMA copolymers functionalized with triphenylphosphonium as drug carriers for membrane transduction and mitochondrial localization. *Biomacromolecules* **2006**, *7* (8), 2347–2356.

(67) Slobbe, R.; Poels, L.; ten Dam, G.; Boerman, O.; Nieland, L.; Leunissen, J.; Ramaekers, F.; van Eys, G. Analysis of idiotope structure of ovarian cancer antibodies: recognition of the same epitope by two monoclonal antibodies differing mainly in their heavy chain variable sequences. *Clin. Exp. Immunol.* **1994**, *98* (1), 95–103.

Table 4. Dose Ratios and IC_{50} Doses in Combinations of Free Drugs (SOS+Mce_6), Nontargeted Copolymer Conjugates (P-GFLG-SOS+P-GFLG-Mce_6), and Targeted Copolymer Conjugates [P-(GFLG-SOS)-Fab′+P-(GFLG-Mce_6)-Fab′] in OVCAR-3 Cells

drug combination			
drug A	drug B	dose ratio	D_m (μM)[a] (dose A + dose B)[b]
SOS	Mce_6	1:1.61	0.096 ± 0.0077 (0.037 + 0.059)
P-GFLG-SOS	P-GFLG-Mce_6	1:0.38	1.69 ± 0.22 (1.22 + 0.47)
P-(GFLG-SOS)-Fab′	P-(GFLG-Mce_6)-Fab′	1:0.031	1.70 ± 0.38 (1.65 + 0.051)

[a] D_m values are the means ± SEM (n = 6 in single experiment). [b] Doses of drug A and drug B were calculated approximately from the D_m of each combination and dose ratio.

***In Vitro* Inhibition of OVCAR-3 Cell Growth with Drug Combinations.** The investigation of possible synergistic, additive, or antagonistic effects of sequential combinations of SOS+Mce_6, P-GFLG-SOS+P-GFLG-Mce_6, or P-(GFLG-SOS)-Fab′+P-(GFLG-Mce_6)-Fab′ against the ovarian carcinoma OVCAR-3 cell line was performed *in vitro* by exposing cells to SOS or its conjugates for 4 days, followed by exposure of cells to Mce_6 or its conjugates for 1 day, and finally, a 30 min irradiation. This sequential combination was chosen because the optimal exposure times of SOS/P-GFLG-SOS/P-(GFLG-SOS)-Fab′ and Mce_6/P-GFLG-Mce_6/P-(GFLG-Mce_6)-Fab′ were different (4 days for SOS and 1 day for Mce_6), as mentioned above. The dose ratios of each combination (Table 4) were based on their respective IC_{50} concentrations from Table 3 as a series of 2-fold dilutions from 4 to 0.03125 times IC_{50}. Figure 4 shows the composite dose−response curves and median-effect plots of OVCAR-3 cells, indicating the antiproliferative effects of single agents and their combinations. The dose−response curves for combined treatment were obtained by plotting % cell viability (y) vs the combined dose of two single agents (x). The median-effect plots of single agents and combinations were derived from the linear part of dose−response curves. All of the combination treatments showed antiproliferative activities toward OVCAR-3 cells. The dose ratio and D_m values of the combination treatments are shown in Table 4. The IC_{50} dose of each drug in combinations was significantly lower than those of each drug as single agents (compare Tables 3 and 4). These results clearly indicate that all of the combination treatments were effective against OVCAR-3 cells.

The CI analysis was used to assess the drug−drug interaction of the sequential combinations of free drugs, nontargeted and targeted copolymer conjugates toward OVCAR-3 cells *in vitro*.[41,42] In the CI analysis, values of CI < 1, CI = 1, and CI > 1 indicate synergy, additivity, and antagonism, respectively. Figure 5 shows the combination index plots (f_a−CI plots) over all inhibition effect levels (f_a = 0.05−0.95 or 5−95% of inhibition effect) in OVCAR-3

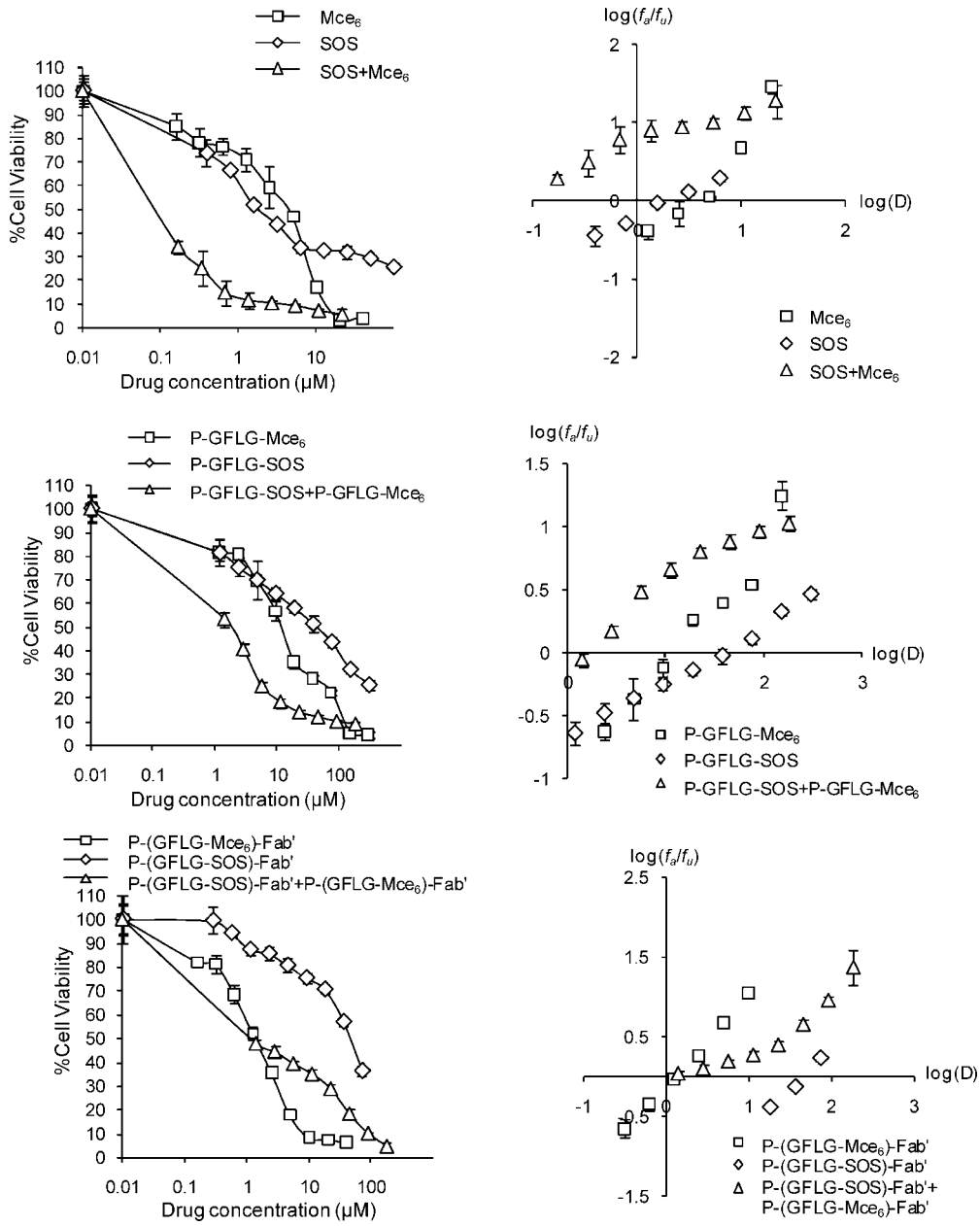

Figure 4. Dose response curves and median-effect plots of OVCAR-3 cells treated with Mce_6, SOS, P-GFLG-Mce_6, P-GFLG-SOS, P-(GFLG-Mce_6)-Fab′, and P-(GFLG-SOS)-Fab′ as single agents and sequential combinations at constant ratios of their respective IC_{50} concentrations. Bars represent standard error ($n = 6$ in single experiment).

cells. The sequential combinations of SOS+Mce_6 and P-GFLG-SOS+P-GFLG-Mce_6 yield CI values lower than 1 over the entire range of cytotoxicity, indicating very strong synergistic to synergistic effects. The P-(GFLG-SOS)-Fab′+P-(GFLG-Mce_6)-Fab′ combination also displayed a strong synergism for f_a values up to about 0.85, but showed synergistic effect and nearly additive effect at $f_a = 0.9$ and 0.95, respectively.

The drug interactions may depend on the differences of drugs in the combination, such as physicochemical properties, the mechanisms of action, and the drug exposure schedules. All these differences may result in different antitumor activities. SOS and Mce_6 are hydrophobic low molecular weight molecules, but both have different mechanisms and sites of action. SOS acts on p53 and DNA while Mce_6 can cause damage to biological molecules by generation of reactive oxygen species. In our previous study, we compared the simultaneous combination of P-GFLG-SOS+P-GFLG-Mce_6 to SOS+Mce_6 against the human renal A498 carcinoma cell line. After 16 h cell exposure to the combinations, both combinations displayed synergism for f_a up to 0.8, but showed slight antagonism and near additivity at $f_a = 0.95$.[31] Many researchers have studied the antitumor activities following different drug exposure schedules. For example, the simultaneous and sequential exposures of irofulven with oxaliplatin or cisplatin against human breast, colon, and ovarian cancer cell lines showed that the sequence oxaliplatin

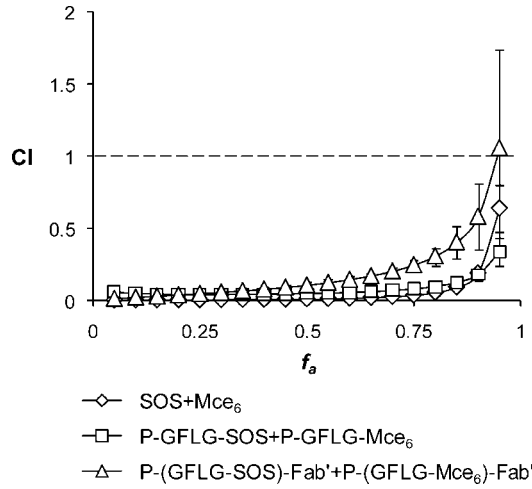

Figure 5. Combination index plots (f_a−CI plots) obtained from median-effect analysis. Chemotherapeutic drugs and their HPMA copolymer conjugates were gradually diluted at the ratio of their IC_{50} values as a series of 2-fold dilutions from 4 to 0.03125 times IC_{50} and OVCAR-3 cells exposed to drugs sequentially as described in Materials and Methods. CI < 1, = 1 and > 1 indicate synergism, additive effect, and antagonism, respectively. The vertical bars indicate the 95% confidence intervals based on sequential deletion analysis (SDA) and can be generated by using CompuSyn software.

followed by irofulven displayed better synergistic effect than the other schedules.[68]

Conclusion

Combination chemotherapy and PDT with free SOS and Mce$_6$, their nontargeted and Fab′-targeted HPMA copolymer conjugates in human ovarian carcinoma OVCAR-3 cells was evaluated. Sequential combinations of these therapeutics produced very strong synergism to nearly additivity in the treatment of OVCAR-3 cells. The synergistic effects ranked in the order P-GFLG-SOS+P-GFLG-Mce$_6$ > SOS+Mce$_6$ > P-(GFLG-SOS)-Fab′+P-(GFLG-Mce$_6$)-Fab′. These data support continued *in vivo* investigations of SOS and Mce$_6$ combinations to determine the antitumor activity for the treatment of ovarian cancer.

Abbreviations Used

AIBN, 2,2′-azobisisobutyronitrile; APMA, *N*-(3-aminopropyl)methacrylamide hydrochloride; CI, combination index; D_m, median-effect dose; DI, deionized; DIPEA, *N,N*′-diisopropylethylamine; DMAP, 4-dimethylaminopyridine; DMF, *N*,*N*-dimethylformamide; DOX, doxorubicin; EPR, enhanced permeability and retention; GFLG, glycylphenylalanylleucylglycine; HPMA, *N*-(2-hydroxypropyl)methacrylamide; IC_{50}, concentration that inhibited cell growth by 50% as compared with control cell growth; MA, methacryloyl; mAb, monoclonal antibody; M_w, weight average molecular weight; Mce$_6$, mesochlorin e$_6$ monoethylenediamine disodium salt; MTT assay, modified 3-(4,5-dimethylthiazol-2-yl)-2,5-diphenyltetrazolium bromide assay; ONp, *p*-nitrophenoxy; P, HPMA copolymer backbone; PDT, photodynamic therapy; P-GFLG-Mce$_6$, HPMA copolymer−Mce$_6$ conjugate; P-(GFLG-Mce$_6$)-Fab′, antibody Fab′ fragment targeted HPMA copolymer−Mce$_6$ conjugate; P-GFLG-ONp, HPMA copolymer precursor containing reactive *p*-nitrophenyl ester groups at side chain termini; P-GFLG-SOS, HPMA copolymer−SOS conjugate; P-(GFLG-SOS)-Fab′, antibody Fab′ fragment targeted HPMA copolymer−SOS conjugate; 5-SFX, 6-(fluorescein-5-carboxamido)hexanoic acid succinimidyl ester; SMCC, succinimidyl *trans*-4-(maleimidomethyl)cyclohexane-1-carboxylate; SOS, 2,5-bis(5-hydroxymethyl-2-thienyl)-furan; THF, tetrahydrofuran.

Acknowledgment. We thank the Drug Synthesis and Chemistry Branch of National Cancer Institute for supplying SOS. The research was supported in part by the NIH grant CA51578 from the National Cancer Institute, and by the Thailand Research Fund (TRF) through the Royal Golden Jubilee Ph.D. Program (Grant No. PHD/0176/2545).

MP800006E

(68) Serova, M.; Calvo, F.; Lokiec, F.; Koeppel, F.; Poindessous, V.; Larsen, A. K.; Laar, E. S.; Waters, S. J.; Cvitkovic, E.; Raymond, E. Characterizations of irofulven cytotoxicity in combination with cisplatin and oxaliplatin in human colon, breast, and ovarian cancer cells. *Cancer Chemother. Pharmacol.* **2006**, *57* (4), 491–499.